Numerical analysis of CdS/PbSe room temperature mid-infrared heterojunction photovoltaic detectors

Binbin Weng, Jijun Qiu, Wanyin Ge, Zhisheng Shi

Binbin Weng, Jijun Qiu, Wanyin Ge, Zhisheng Shi, "Numerical analysis of CdS/PbSe room temperature mid-infrared heterojunction photovoltaic detectors," Proc. SPIE 9451, Infrared Technology and Applications XLI, 945116 (4 June 2015); doi: 10.1117/12.2175813

SPIE.

Event: SPIE Defense + Security, 2015, Baltimore, Maryland, United States

Numerical analysis of CdS/PbSe room temperature mid-infrared heterojunction photovoltaic detectors

Binbin Weng[a*], Jijun Qiu[a], Wanyin Ge[a], and Zhisheng Shi[a, b*]
a. The School of Electrical & Computer Engineering, University of Oklahoma, Norman, Oklahoma 73019 USA
b. Nanolight Inc., Norman, Oklahoma 73069 USA
* E-mail: binbinweng@ou.edu; shi@ou.edu

ABSTRACT

Numerical analysis of a CdS/PbSe room-temperature heterojunction photovoltaic detector is discussed as to provide guidelines for practical improvement, based on the previous experimental exploration [1]. In our experiment work, the polycrystalline CdS film was prepared in hydro-chemical method on top of the single crystalline PbSe grown by molecular beam epitaxy method. The preliminary results demonstrated a 5.48×10^8 Jones peak detectivity at λ=4.7μm under zero-bias. However, the influence of some material and device parameters such as carrier concentration, interface recombination velocity remains uncertain. These parameters affect the built-in electric field and the carriers' transportation properties, and consequently could have detrimental effect on the device performance of the CdS/PbSe detector. In this work, therefore, the numerical analysis is performed based on these parameters. The simulation results suggest that the device performance can be improved at least 4 times by increasing CdS concentration for two orders of magnitudes, and the device performance will degrade severely if the interface recombination speed is over 10^4 cm/s.

Keywords: lead salt, uncooled, heterojunction, and mid-infrared photovoltaic detectors.

1. INTRODUCTION

Mid-infrared detectors working in the range between 3-5μm and 8-12μm have been drawing widely attentions in research, industrial and military fields for decades, due to the facts that they can be used for the applications such as gas analysis, thermal imaging and so on. In recent years, there is a rapid growing market demand for the mid-infrared detectors working at room temperature, majorly because thermal imaging cameras built with such detectors are much less expensive and more compact than the one that needs to be cryogenic cooled. So far, the microbolometer-based cameras made out of Vanadium Oxide (VO_x) or Amorphous Silicon (α-Si) dominate the commercial market world widely, which are generally used for human body detection. This type of detectors is a thermal sensor that absorbs the infrared radiation and changes the temperature of the VO_x or α-Si materials, and the resulting change in the internal electrical polarization is used to generate an electrical output. They are compact, low power required, and relatively cheap. However, there are two major limits for

Infrared Technology and Applications XLI, edited by Bjørn F. Andresen, Gabor F. Fulop, Charles M. Hanson, Paul R. Norton, Proc. of SPIE Vol. 9451, 945116 · © 2015 SPIE · CCC code: 0277-786X/15/$18 · doi: 10.1117/12.2175813

this type of detectors. Firstly, the response speed is slow (typical response time for VO_x is 45 ms and for α-Si is 21 ms), [2, 3] majorly because the heating and cooling of the detector element is a relatively slow process. Secondly, due to the fact that the sensitivity of thermal detectors is limited by the thermal conductance of the pixel, it is less sensitive than photodetector imagers. Instead, in a photodetector, the infrared radiation is absorbed by a photon quantum process, thus solving the problem associated with thermal detectors. However, for current semiconductor mid-infrared photodetectors, Auger recombination is the major loss channel at high temperature and thus is the key hurdle for their development. It is known that Auger coefficient in Pb-salt materials [4, 5] is more than an order of magnitude lower than those in type-II QWs, [6] which are significantly suppressed compared to other III-V and II-VI semiconductors with the same energy band gaps. Therefore, PbSe material is the major player in the current uncooled photodetectors market. Furthermore, the room temperature operating PbSe photoconductive detectors made by our group have demonstrated significantly improved specific detectivity (D*) of 2.8×10^{10} cm·Hz$^{1/2}$/W [7] and 4.2×10^{10} cm·Hz$^{1/2}$/W [8] at ~3.8 μm, without and with antireflective coating.

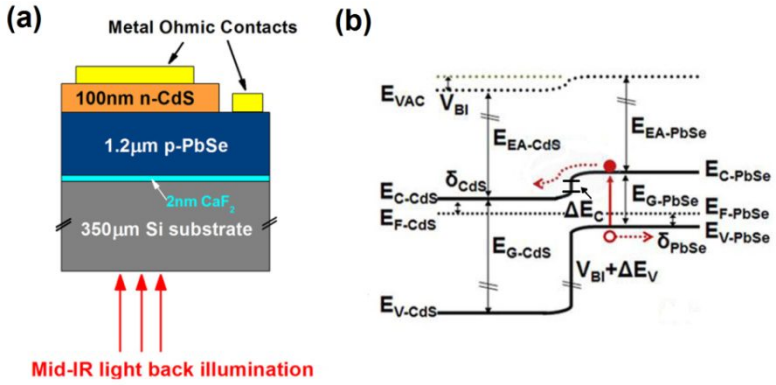

Figure 1. (a) Schematic of the CdS/PbSe heterojunction photodetector; (b) Energy band diagram of n-CdS/p-PbSe heterojunction photodetector.

Nevertheless, in terms of photovoltaic (PV) type Pb-salt detectors, this advantage of low Auger recombination has not been fully explored, which is partially due to the lack of good junctions with low dark current. Previous research works on PV Pb-salt detectors have been mainly focused on using Pb/Pb-salt Schottky junctions. [9, 10] The performance of such detectors is still far below the theoretical limit of Auger recombination. But the performance enhancement is possible by the Pb-salt material quality improvement [11, 12] or the device junction engineering. For the latter one, it has been shown that replacing Schottky contact by p-n homojunction can outperform their Schottky counterparts. [13, 14] Furthermore, by constructing a larger band gap semiconductor with Pb-salt material to form p-n heterojunction with proper band offsets will be able to offer even higher R_0A values by allowing minority carrier transport and blocking the majority carrier leak. Therefore, finding

a proper semiconductor material to form a good heterojunction with Pb-salts is critical for device performance improvement.

CdS is a wide band gap semiconductor material with Eg at ~2.4 eV and has been widely known as a n-type and window material in high efficiency thin film solar cells based on CdTe and Cu(In, Ga)Se_2. [15, 16] The electron affinity of CdS reported [17] is very close to PbSe material. From this point of view, CdS has the potential to form a good heterojunction with PbSe film for mid-IR photodiode detector fabrication. Therefore, a preliminary experimental exploration on the feasibility of using CdS/PbSe heterostructure for mid-IR detector applications has been investigated and reported by our group recently. [1] The device demonstrated the preliminary performance at room temperature with 55mA/W peak responsivity and 5.48×10^8 Jones peak detectivity at λ=4.7μm under zero-bias photovoltaic mode.

The preliminary experimental results are promising, but the effects of some material and device parameters including carrier concentration, and interface recombination states still remain unclear. And those two parameters have direct influences on the built-in electric field and the carriers' transportation properties. Therefore, in order to figure out the impact of these parameters to the device performance, and also provide some basic theoretical guidelines to help improve the experimental result, in this work, the numerical analysis will be performed.

2. DEVICE MODELING & SIMULATION SETUP

In this work, a one dimensional simulation program called SCAPS, is used for the n-CdS/p-PbSe heterojunction photodetector structure. Figure 1(a) shows the schematic structure of the CdS/PbSe heterostructure on double side polished Si wafer, in which PbSe is single-crystalline grown by Molecular Beam Epitaxial method (MBE) and CdS is poly-crystalline synthesized by the Chemical Bath Deposition method (CBD). Figure 2(a) shows the energy band diagram for the heterojunction structure, which is suggested to be a type II alignment heterojunction according to the work shown in the previous work. [1]

The working mechanism of the heterojunction can be described as follows. When light of mid-infrared wavelength (3-5μm) falls onto the heterojunction photodetector in back-illumination mode, the light induced electron-hole pairs will be generated mostly in neutral p region of PbSe layer. When these carrier pairs diffuse to the depletion region of the junction, they will be separated and collected due to the built-in electric field as shown in Figure 1(b), and the photocurrent will get generated consequently.

After defining the physical structure of the device, fundamental material properties of CdS and PbSe are also provided as listed in Table 1, including the values of bandgap, relaive

permittivity, effective mass of electrons and holes, doping concentrations, carrier mobilities, radiative recombination coefficient, auger recombination coefficient and electron affinity. Other parameters required for simulation such as density of states for electrons in conduction band (N_c) and for holes in valence band (N_v) have been calculated using following formulas:

$$\begin{cases} N_C = 2\left[2m_e^* kT/h^2\right]^{3/2} n \\ N_V = 2\left[2m_h^* kT/h^2\right]^{3/2} n \end{cases},$$

in which n stands for the degeneration factor. It is 1 for CdS and 4 for PbSe due to the energy bands degeneration reason.

Table 1. Values of room temperature parameters used for the simulation of CdS/PbSe photovoltaic detector.

Parameters @300K	**CdS**	**PbSe**
Energy band gap (Eg)	2.4eV	0.28eV
Relative Permittivity (ε)	5.7	23
Effective mass of electrons (m_e^*)	$0.21m_0$	$0.079m_0$
Effective mass of holes (m_e^*)	$0.80m_0$	$0.066m_0$
Donor concentration (N_D)	1×10^{16}~1×10^{18} cm^{-3}	N/A
Acceptor concentration (N_A)	N/A	$3\times10^{17}cm^{-3}$
Electron Mobility (μ_n)	~1 cm^2/Vs	400 cm^2/Vs
Hole Mobility (μ_p)	~0.24 cm^2/Vs	500 cm^2/Vs
Radiative recombination coefficient	1×10^{-10} cm^3/s	3.45×10^{-11} cm^3/s
Auger recombination coefficient	-	6.49×10^{-28} cm^3/s
Electron Affinity (E_A)	4.5eV	4.5eV
Thickness	100nm	1.2μm

In prior to the simulation work, there are some assumptions and notes need to be addressed. Firstly, the doping concentrations are assumed to be uniform for all the regions in the materials. Secondly, the top and bottom contacts are assumed to be ohmic. Although, in practice, there is generally a small schottky barrier at the metal contacts which results in degradation of fill factor and the open circuit voltage. Thirdly, since there is no conclusive quantitative result of the ΔE_c reported before, in order to simplify the discussion process, it is assumed to be zero to flatten up the conduction bands of CdS and PbSe in the simulation. It is necessary to note that, since the single crystalline PbSe film is grown by molecular beam epitaxy, most material parameters in PbSe film has been optimized and stabilized, including the doping concentration and carrier mobility. Therefore, the simulation parameters will be focusing on either CdS side or the interface between CdS and PbSe films. Last but not least, for the simulation, three basic types of recombination in the bulk of semiconductor including

band-to-band radiative, Auger and Shockley-Read-Hall recombination mechanisms will all be considered.

3. RESULTS AND DISCUSSION

3.1 CdS Carrier Concentrations

In our reported experimental exploration work, the carrier concentrations of CdS and PbSe thin films prepared were determined to be n~1×10^{16} cm^{-3} and p~3×10^{17} cm^{-3} respectively by Hall effect measurements in Van der Pauw four-point probe configuration. It is known that the depletion width (x_p and x_n) and the built-in potential (V_{PbSe} and V_{CdS}) of a space charge region are different in the adjunct materials of the heterojunction, due to the difference of dielectric constant and doping concentrations as shown in the expression below.

$$\begin{cases} V_{CdS}/V_{PbSe} = (\varepsilon_{PbSe} N_A)/(\varepsilon_{CdS} N_D) \\ x_p N_A = x_n N_D \end{cases}.$$

Especially, in this case, because the dielectric constant of PbSe is greatly higher than CdS, and the material parameters of PbSe have been optimized and fixed experimentally, the doping concentration of CdS becomes very critical parameter to be tuned and will affect the built-in electric field in the junction, eventually the performance of the device.

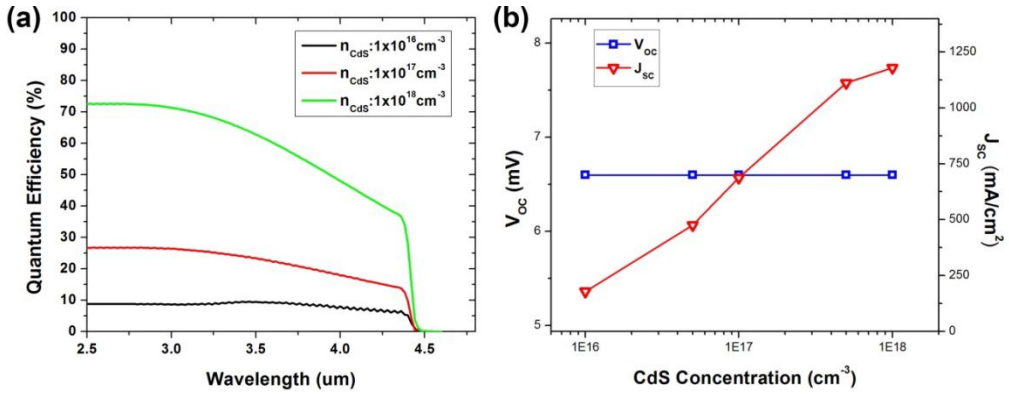

Figure 2. CdS electron concentration dependent (a) spectral quantum efficiency and (b) open circuit voltages & short circuit current density of the CdS/PbSe photovoltaic detector.

In the simulation for this section, the hole concentration of PbSe is set at 3×10^{17} cm^{-3}, and the minority lifetime τ is assumed to be ~1ns based on the reported experimental result. It is noted that since the Auger recombination in the PbSe epitaxial film grown on Si is of orders magnitude lower than SRH recombination, the minority carrier lifetime is set by controlling the SRH lifetime, and therefore it majorly reflects the SRH recombination process in the PbSe material. And the interface states recombination speed is set at 1×10^4 cm/s which will be introduced and investigated in the next section.

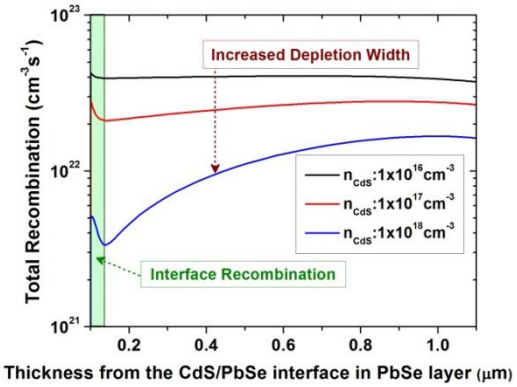

Figure 3. The total recombination profile in the PbSe side of the heterojunction structure

Figure 2 shows the device performance depending on the different CdS concentrations, including (a) spectral dependent quantum efficiency, (b) short circuit current density and open circuit voltage. In figure 2 (a), according to the experiment data, the black line presents the result with the CdS concentration at 1×10^{16} cm^{-3} which is of <10% efficiency. However, as we mentioned previously, since the CdS concentration is over one magnitude lower than the PbSe one, most of the space charge area locates in CdS side based on the equation $x_p N_A = x_n N_D$. In this case, almost all light generated excess carriers are in the neutral PbSe area and have to be collected by diffusing to the depletion region. There are two major drawbacks: 1. Limited by the short diffusion length, the contributions of the photocurrents are not effective; 2. the diffusion process is slow which results in a slow photoresponse if the optical intensity varies with time. Therefore, in order to reduce the influence of the drawback mentioned, it is necessary to increase the concentration up for one to two orders of magnitude, and consequently the depletion width will extend into the PbSe layer. As shown in Figure 2 (a), after increasing the concentration, the quantum efficiency increases largely which is predominately due to the improvement of the short circuit current density as shown in Figure 2(b) and is also an indicator of the enhanced minority carrier collection efficiency. The major reason for the enhancement can be explained as follows: the built-in electric field extends into p-side due to the increased CdS electron concentration, and then depletes more area in the PbSe active layer, consequently it will greatly reduce all the carrier concentration dependent recombination mechanisms as shown in figure 3, including radiative, Auger and SRH process in this depleted area based on the general recombination equation in a semiconductor shown as follows:

$$R_{total} = r_{rad} np + r_{Aug-e} n^2 p + r_{Aug-h} np^2 + \frac{n}{\tau_{SRH-e}} + \frac{p}{\tau_{SRH-h}},$$

where R_{total} is total recombination rate, r_{rad} is radiative recombination coefficient, n is electrons concentration, p is holes concentration, r_{Aug-e} and r_{Aug-h} are the Auger carriers

recombination coefficients, $\tau_{SRH\text{-}e}$ and $\tau_{SRH\text{-}h}$ are the carriers lifetimes of SRH recombination respectively. By the way, in figure 3, the sudden increase of the recombination in the green color marked area close to the interface between CdS and PbSe is caused by the interface recombination states.

Therefore, under this circumstance, it is clear that more net photon generated minority carriers can be collected. From this perspective, the device performance can be largely improved if the CdS concentration can be alleviated by at least one order of magnitude in practical experiments.

3.2 Interface States Recombination

It is known that the interface recombination processes can significantly alter the device performance especially for heterojunctions due to several reasons, such as lattice mismatch, thermal mismatch, different crystal orientation, and different crystal formation etc. In this work, the effect of interface quality on the device performance is modeled by the interface recombination velocity S_i. It is noted that the charge type of the interface state is defined as acceptor-like defects locating ~50meV below the conduction band (~2 times larger than the thermal energy k_BT ~ 26meV) spreading uniformly over the whole interface between CdS and PbSe, which majorly contribute to the minority carrier loss since the p-type PbSe material is the only active layer responsible for light absorption. To determine the effect of the interface recombination velocity on the device performance, S_i is then varied from 10^0 cm/s to 10^7 cm/s. And in this simulation section, the CdS concentration is set at 1×10^{17} cm^{-3}.

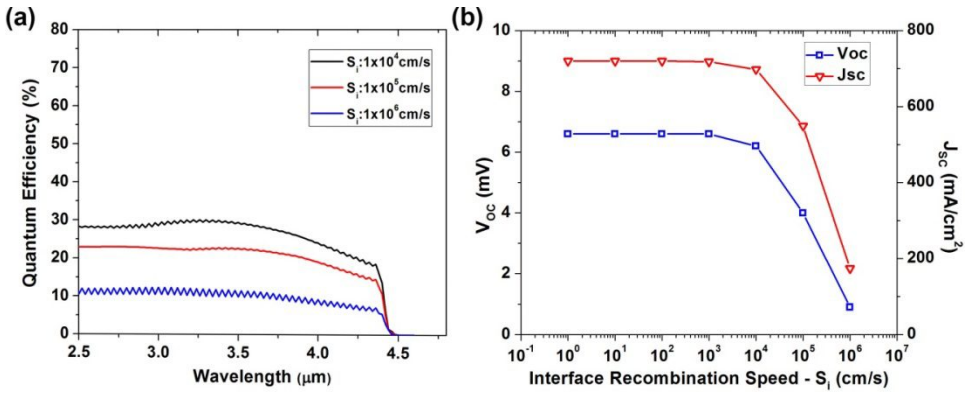

Figure 4. Recombination rate of interface states dependent dependent (a) spectral quantum efficiency and (b) open circuit voltages & short circuit current density of the CdS/PbSe photovoltaic detector.

Figure 4 shows the device performance depending on the different CdS/PbSe interface recombination speeds, including (a) spectral dependent quantum efficiency, (b) short circuit current density and open circuit voltage. It is clearly visible from figure 3(b) that the device performance is not strongly affected by the interface recombination speed if it is below 10^4

cm/s. However, when S_i increases above 10^4 cm/s, both short circuit current density and open circuit voltage degraded quickly, and consequently makes spectral quantum efficiency drops largely as shown in figure 4 (a).

This trend is obvious because high interface states in the depletion region can kill a large amount of excess minority carriers while they are on the process of swept through the junction by the electric field. It has been mentioned that the CdS film was grown by using chemical bath deposition method at around 70~80^{o}C directly on PbSe single crystalline film. And the CdS layer grown was polycrystalline indicated by the scanning electron microscope characterization, and the structure was predominant by the zinc blend form measured by powder X-ray diffraction (XRD). Without any post treatment, the low quality interface between CdS and PbSe can be easily expected in this case. So it is reasonable to suggest that the interface recombination velocity in that device is at the range above 10^4 cm/s. Therefore, it is also able to improve the device performance by improving the interface quality to make S_i decreasing down below 10^4 cm/s.

4. CONCLUSION

To sum up, two factors including CdS electron concentration and the interface recombination rate between CdS and PbSe have been discussed numerically by using 1-D photovoltaic simulation software, in order to provide some guidelines to help improve the performance of the proposed room temperature CdS/PbSe photovoltaic mid infrared detector experimentally. It is found that by increasing the concentration of CdS film by two orders of magnitudes, the device performance can be improved at least 4 times. And the strong impact of the high interface recombination rate also suggests that to improve the interface quality by modifying the growth method or post annealing treatment is very important and critical experimentally.

ACKNOWLEDGMENTS

We acknowledge financial supports from the DoD AFOSR under Grant No. FA9550-12-1-0451, DOD ARO Grant No. W911NF-07-1-0587, and Oklahoma OCAST program under Grant Nos. AR112-18 and AR132-003.

REFERENCES

[1] Weng, B., Qiu, J., Zhao, L., Chang, C., and Shi, Z., "CdS/PbSe heterojunction for high temperature mid-infrared photovoltaic detector applications," Applied Physics Letters 104, 121111 (2014)

[2] Capper, P., Elliottm, C.T., "Infrared Detectors and Emitters: Materials and Devices," Kluwer Academic Publishers, (2001)

[3] Tissot, J. L., Legras, O., Trouilleau, C., Crastes, A., and Fieque, B., "Uncooled microbolometer detector: recent development at ULIS," Proc.SPIE 5987, 200-210 (2005)

[4] Klann, R., Hofer, T., Buhleier, R., Elsaesser, T., and Tomm, J. W., "Fast recombination processes in lead chalcogenide semiconductors studied via transient optical nonlinearities," J. Appl. Phys. 77, 277 (1995)

[5] Findlay, P. C., Pidgeon, C. R., Kotitschke, R., Hollingworth, A., Murdin, B. N., Langerak, C. J. G. M., van der Meer, A. F. G., Ciesla, C. M., Oswald, J., and Homer, A., et al, "Auger recombination dynamics of lead salts under picosecond free-electron-laser excitation," Phys. Rev. B 58, 12908 (1998)

[6] Meyer, J. R., Felix, C. L., Bewley, W. W., Vurgaftman, I., Aifer, E. H., Olafsen, L. J., Lindle, J. R., Hoffman, C. A., Yang, M.-J., and Bennett, B. R., et al, "Auger coefficients in type-II InAs/$Ga_{1-x}In_xSb$ quantum wells," Appl. Phys. Lett. 73, 2857 (1998)

[7] Qiu, J., Weng, B., Yuan, Z., and Shi, Z., "Study of sensitization process on mid-infrared uncooled PbSe photoconductive detectors leads to high detectivity," J. Appl. Phys. 113, 103102 (2013).

[8] Weng, B., Qiu, J., Yuan, Z., Larson, P., Strout, G., and Shi, Z., "High respsonsivity enhancement of mid-infrared PbSe detectors using CaF_2 nano-structural antireflective coatings," Appl. Phys. Lett. 104, 021109 (2014)

[9] Hohnke, D. K., Holloway, H., "Epitaxial PbSe Schottky-barrier diodes for infrared detection," Appl. Phys. Lett., 24, 633 (1974)

[10] Zogg, H., Fach, A., John, J., Masek, J., Muller, P., Paglino, C., and Blunier, S., "Photovoltaic IV-VI on Si infrared sensor arrays for thermal imaging," Optical Engineering 34, 1964-1969 (1995)

[11] Muller, P., Zogg, H., Fach, A., John, J., Paglino, C., Tiwari, A. N., and Krejci, M., "Reduction of threading dislocation densities in heavily lattice mismatched PbSe on Si (111) by glide," Phys. Rev. Lett. 78, 3007-3010 (1997)

[12] Weng, B., Zhao, F., Ma, J., Yu, G., Xu, J., and Shi, Z., "Elimination of threading dislocations in as-grown PbSe film on patterned Si (111) substrate using molecular beam epitaxy," Appl. Phys. Lett. 96, 251911 (2010)

[13] Gupta, S. C., Sharma, B. L., and Agashi, V. V., "Comparison of schottky barrier and diffused junction infrared detectors," Infrared Physics, 19, 545-548 (1979)

[14] Zogg, H., Fach, A., Maissen, C., Masek, J., and Blunier, S., "Photovoltaic lead-chalcogenide on silicon infrared sensor arrays," Optical Engineering, 33, 1440-1449 (1994)

[15] Ferekides, C. S., Marinskiy, D., Viswanathan, V., Tetali, B., Palekis, V., Selvaraj, P., and Morel, D. L., "High efficiency CSS CdTe solar cells," Thin Solid Films 361-362, 520-526 (2000)

[16] Orgassa, K., Rau, U., Nguyen, Q., Schock, H. W., and Werner, J. H., "Role of the CdS buffer layer as an active optical element in Cu (In, Ga) Se_2 thin film solar cells," Progress in Photovoltaics: Research and Applications 10, 457-463 (2002)

[17] Brus, L. E., "A simple model for the ionization potential, electron affinity, and aqueous redox potentials of small semiconductor crystallites," the Journal of Chemical Physics 79, 5566 (1983)